Absolute phase mapping for one-shot dense pattern projection

Sergio Fernandez, Joaquim Salvi

Institute of Informatics and Applications, Univ.Girona

Av. Lluis Santalo S/N, E-17071 Girona (Spain)

sergiofn, qsalvi@eia.udg.edu

Tomislav Pribanic

Faculty Electrical Engineering and Computing, Univ.Zagreb

Unska 3, HR-10000, Zagreb (Croatia)

Tomislav.Pribanic@fer.hr

Abstract

The use of one-shot pattern projection to obtain 3D dense reconstruction constitutes a promising field of research in structured light. Most of the related works presented in the literature are based on the projection of a fringe pattern to extract depth from phase deviation. However, the algorithms employed to unwrap the phase are computationally slow and can fail under certain slopes and occlusions in the object shape. In these lines, a color one-shot dense reconstruction using fringe pattern projection and wavelet decomposition is presented. Moreover, a novel phase unwrapping algorithm is proposed, providing a fast and reliable absolute phase map for depth reconstruction.

1. Introduction

Three dimensional reconstruction using structured light constitutes an active topic in computer vision, having different applications such as range sensoring, industrial inspection, reverse engineering, object recognition, 3D map building, biometrics and others. Within them, applications requiring dense reconstruction with real time response have increased during the last years due to the necessity to deal with dynamic scenarios. Some proposals have been done using fast capturing cameras and a set of projection patterns. However, the ability to work in real time conditions regardingless the speed of motion (up to the acquisition time required by the camera) is only achieved by one-shot projection techniques. Moreover, absolute coding represents a must for most of the applications mentioned above. Different techniques using De Bruijn codes and M-arrays have been developed [15], [5], [11], [12], obtaining a sparse reconstruction with absolute coding and good accuracy results. In contrast, the use of one-shot projections to obtain dense reconstruction having absolute coding has not been studied that much. Some techniques combining one-shot projection and absolute coding were proposed by Carrihill and Hummel [3] and Tajima and Iwakawa [19]. They present a grayscale pattern and a rainbow pattern coded in spatial domain. However, as stated by Salvi et al. [16], they suffer from low resistance to noise and low level of accuracy. In order to obtain better reconstruction results more information must be embedded in the pattern. That is, the amount of information that could be obtained from a set of projections must be condensed to one single shot. To this end, a multiplexation of patterns in frequency or color space is required. The algorithm proposed in this paper utilizes the ideas of dense reconstruction combined with a novel method for phase unwrapping in order to obtain a one-shot dense reconstruction having absolute coding. The paper is structured as follows: section 2 presents a brief overview on dense reconstruction methods, while section 3 introduces the absolute coding unwrapping algorithm. The design of the method is presented in section 4, and the experimental results with both simulated and real data are presented in section 5. Finally, section 6 concludes with a discussion of the proposed method, analyzing the advantages and disadvantages and pointing out the line of research for future work.

2. Brief overview of dense reconstruction techniques

Dense reconstruction refers to the ability of obtaining a full resolution 3D model of the analyzed scenario. This feature has been usually accomplished by using a continuous pattern. These patterns, named as continuous coding strategies, show a continuous intensity or color variation throughout the coding axis [17]. Different continuous approaches have been proposed in the literature, the majority of them using a fringe pattern with both trapezoidal or sinousoidal shape. Within them, sinusoidal strategies present lower errors due to defocusing [7] and are easier to analyse by a transformation to frequency domain. The 3D information obtained from the projection is stored as a phase deviation of the sinusoidal fringe, which is extracted using a proper phase extraction algorithm. Some of the approaches used in the literature for dense reconstruction include Phase Measurement Profilometry (PMP), Fourier Transform Profilometry (FTP) and, more recently, Wavelet Transform Profilometry (WTP).

Phase Measurement Profilometry (PMP) was firstly proposed by Srinivasan et al. [18]. The idea of this technique is to create a set of sinusoidal patterns which are pro-

jected and shifted over time. Every projection is shifted from the previous projection by a factor of $2\pi/N$, being N the total number of projections. From the deformation caused to the set of projected sinusoidal patterns, the object shape is recovered. It is important to mention that this algorithm requires a minimum of $N = 3$ pattern projections to correctly extract the phase deviation. The projected pattern is therefore:

$$I_n^p(y^p) = A^p + B^p cos(2\pi f \cdot y^p - 2\pi n/N) \quad (1)$$

where A^p and B^p are the projection constants, f the frequency of the fringes and y^p the coding axis, $n = 0, 1, ...N$ (superindex p refers to projected pattern). The received intensity values from the object surface, once the set of patterns is projected is:

$$I_n(x, y) = \alpha(x, y)\,[A + Bcos(2\pi f y^p + \phi(x, y) - 2\pi n/N)] \quad (2)$$

where $\alpha(x, y)$ is the different albedo and $\phi(x, y)$ represents the phase deviation introduced by the object shape. It turns out necessary to cancel the effect of different albedo in order to correctly extract the phase deviation. This is performed as shown in eq. (3):

$$\phi(x, y) = \arctan\left[\frac{\Sigma_{n=1}^{N} I_n(x, y) sin(2\pi n/N)}{\Sigma_{n=1}^{N} I_n(x, y) cos(2\pi n/N)}\right] \quad (3)$$

From a minimum of three projected shifted patterns is possible to create a relative phase map and to reconstruct the phase deviation caused by the object shape. However, the arctangent function returns values between the range $(-\pi, \pi]$ and therefore a phase unwrapping procedure is necessary to work with a non-ambiguous phase value out of the wrapped phase. Under real conditions, the required number of projections becomes much more than the theoric minimum of three projections [13], limiting the aplications to static scenarios only.

Fourier Transform Profilometry (FTP) came to cope with this limitation, allowing a faster dense reconstruction compared to PMP. FTP employs the frequency domain to suppress the background component of the recovered pattern. Therefore, one single projection is enough to suppress the different albedo and extract the phase deviation. FTP was first proposed by Takeda and Mutoh [20], and different variations have been proposed since then [8], [4], [22]. The received signal (eq.(2)) is first filtered in frequency and then the phase component can be extracted, as shown in eq. (4)(5)(6):

$$I(x, y) = a(x, y) + c(x, y)e^{2\pi i f y} + c*(x, y)e^{-2\pi i f y} \quad (4)$$

where

$$c(x, y) = \frac{1}{2} b(x, y) e^{i\phi(x,y)} \quad (5)$$

and $c*(x, y)$ is the conjugated value of $c(x, y)$. Finally, the phase component $\phi(x, y)$ was extracted from the imaginary part of eq. (6):

$$log[c(x, y)] = log[(\frac{1}{2})b(x, y)] + i\phi(x, y) \quad (6)$$

The relative phase map $\phi(x, y)$ can be then used as an input to a proper phase unwrapping algorithm. Other FTP techniques have been implemented using 2D Fourier decomposition, which provides better separation of the desired information from noise when dealing with coarse objects [9]. However, most of the sources of noise come from the non-spatial stationarity of the images. Theoretically speaking, Fourier decomposition performs optimally when working with stationary signals, which is not the case for pattern analysis. As a consequence of their limited spatial dimensions, projected patterns suffer from intensity changes due to surface discontinuities. This causes the frequency harmonics to interfere with the first frequency harmonic, making impossible to extract the frequencies around the first harmonic without errors. This effect is known as leackage distortion, and it manifest itself in the form of large errors which occur at the borders of the reconstructed phase map. Also, the existence of any holes in the fringe pattern produces errors that are widespread over the whole fringe patterns image. Moreover, the albedo can interfere into the first harmonic information. The Windowed Fourier Transform (WFT) was proposed to solve this problem, windowing the signal and splitting it into segments before the analysis in frequency domain. The size of this window must be small enough to reduce the errors introduced by boundaries, holes and background illumination, at the same time it must be big enough to hold some periods and hence detect the main frequency and perform an optimal filtering. Sometimes, however, this tradeoff is difficult to achieve and noise arises due to an erroneus frequency detection or to the effect of boundaries.

More recently, the **Wavelet Transform Profilometry** (WTP) was proposed as the solution to the tradeoff present in WFT, as it is able to remove the background illumination and prevent the propagation of errors produced during the analysis, which remain confined in the corrupted regions alone [6]. Additionally, leackage effects in the wavelet transform are much smaller than those evident in the Fourier Transform; consequently, the distortions that occur at the edges of the reconstructed phase maps are largely reduced. This is done by adapting the window width to the frequency that is going to be analyzed [6]. Different methods to analyse the received pattern have been proposed using one dimensional (1D) and two dimensional (2D) wavelet decomposition. The complex wavelet transform (CWT) is usually

used to extract the phase of the received signal [10]. The 1D-CWT algorithm analyses the fringe pattern on a row by row basis. The main concept of the 1D-CWT is to project a row of a fringe pattern onto a family of elementary functions, called the daughter wavelets, which are obtained by both translating and dilating a single basis function, called the mother wavelet. The 2D-CWT algorithm is an extension of the analysis to the two dimensional space. In this case, the daughter wavelets are obtained by translation, dilation and rotation of the mother wavelet. Once the analysis has been performed and the pairs complex wavelet coefficients have been obtained, the next step is to select the most probable coefficient within all the possibilities given by the different daughter wavelets, for every pixel. This process is called phase extraction. There are two main methods for phase extraction, namely the **phase estimation** and the **frequency estimation** approaches. In the phase estimation technique, the optimal phase value is selected from the maximum of the modulus of the wavelet coefficient (for the different scale, translation and rotation values). This provides the most probable daughter wavelet, and its corresponding angle value is selected. An optional cost function can be applied to find the optimal angle values of a pixel taking into account the angle values of the neighbouring pixels. In frequency estimation technique the exact daughter wavelet is extracted from the maximum of the modulus, as in phase estimation techniques. This value can be seen as the instantaneous frequency, which is integrated to obtain the approximated phase value for the given pixel. A complete unwrapped phase distribution is obtained as a result, without the necessity to perform any phase unwrapping algorithm. Unfortunately, this technique provides much worse results than the phase estimation technique, as proved in the work of Abdulbasit [1]. Another important parameter refers to the daughter wavelet used for the decomposition. Some mother wavelet have been tested in the aforementioned work, and the best results in terms of accuracy and resistance to noise are obtained using a Morlet wavelet.

3. A novel proposal for phase unwrapping

As seen before, most of the dense reconstruction algorithms require an unwrapping step to correctly unwrap the phase and extract the object depth. Under absence of noise, if all phase variation between neighbouring pixels is less than π, the phase unwrapping procedure can be reduced to add the corresponding multiple of 2π when a discontinuity appears. Unfortunately, noise, local shadows, under-sampling, fringe discontinuities and irregular surface brightness make the unwrapping procedure much more difficult to solve [16]. Plenty of approaches have been presented in the literature to solve this problem ([21],[2],[6]). However, they usually require a high computational cost and can fail into errors when the surface present a slope like the one shown in Fig. 1. A novel method to overcome this problem is based on the remainder theorem [14], where an absolute phase map can be computed from two different relative phase maps having frequencies that are relative prime numbers between them. Having two relative phase maps with different frequencies and their corresponding phase values $\phi 1$, $\phi 2$ (Fig. 2), the absolute phase value is given by eq. (7):

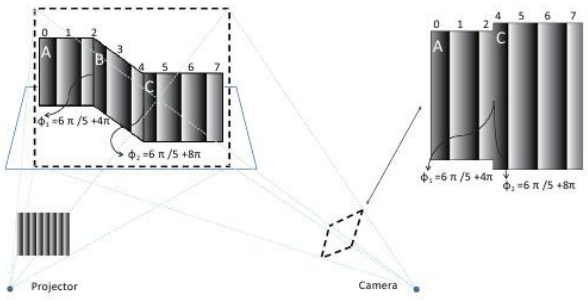

Figure 1: Slope producing decoding error in the traditional fringe pattern methods

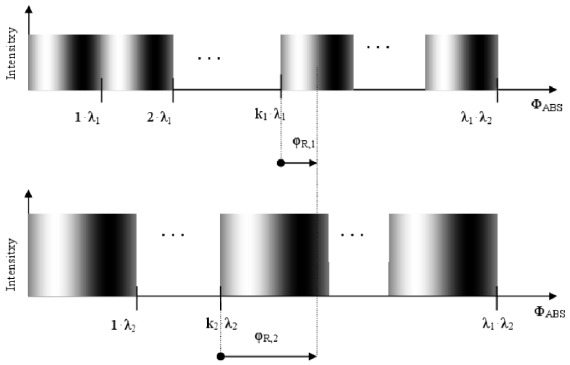

Figure 2: Pair of two different relative phases

$$\Phi_{ABS1,INT} = \Sigma_{k=1}^{N} \phi_{Ri,INT} e_i mod(\lambda_1 \lambda_2) \qquad (7)$$

being λ_i the period wavelengths and e_i a number which divided by λ_i yields a remainder 1, and 0 otherwise (see the work of Pribanic et al. [13] for more details). A solution to $\Phi_{ABS1,INT}$ can be obtained using the previous equation, providing an absolute phase map from a minimun of two relative phases. Another advantage of this technique relies on its simplicity and non dependence on the neighbouring pixels, as the phase value is computed directly from a linear combination of the two relative phase map values for the given pixel.

4. System proposal

Our model proposal employs one-shot color multiplexation, wavelet analysis and absolute coding. The creation and the decoding diagrams are shown in Figs.3,4. A further explanation of the pattern creation and the decoding algorithm is presented in sections 4.1 and 4.2, respectively.

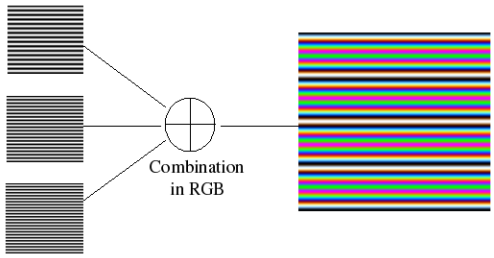

Figure 3: Pattern creation diagram

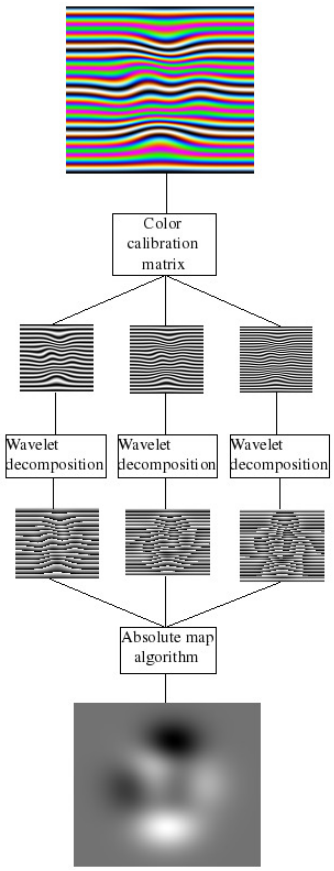

Figure 4: Pattern decoding diagram

4.1. Pattern creation

This pattern is created by multiplexing three different fringe patterns in color space, taking advantage of the Red Green and Blue splitted channels of the projector and camera devices. The frequencies used to create the fringe patterns are relative prime numbers between them. The sinusoidal patterns use one axis coding, as in other WTP approaches. The projected pattern is represented by eq. (8), where A_i, B_i and f_i represent the DC and AC components and the frequency values for every channel (r, g and b):

$$\begin{aligned} I_n^p(y^p) &= A_r^p + B_r^p cos(2\pi f_r y^p) + \\ & A_g^p + B_g^p cos(2\pi f_g y^p) + \\ & A_b^p + B_b^p cos(2\pi f_b y^p) \end{aligned} \quad (8)$$

4.2. Pattern analysis

Once projected onto the pattern and captured by the camera, the received pattern can be represented as:

$$\begin{aligned} & I_n(x,y) = \\ & \delta(x,y) \cdot (\alpha(x,y) \cdot (A_r^p + B_r^p cos(2\pi f_r y^p + \phi(x,y))) + \\ & \beta(x,y) \cdot (A_g^p + B_g^p cos(2\pi f_g y^p + \phi(x,y))) + \\ & \gamma(x,y) \cdot (A_b^p + B_b^p cos(2\pi f_b y^p + \phi(x,y)))) \end{aligned} \quad (9)$$

where $\delta(x,y)$ represent the different albedo and $\alpha(x,y)$, $\beta(x,y)$ and $\gamma(x,y)$ the effect of crosstalk between the different color channels. The first task is to split the three color channels obtained from the camera and perform a color enhancement to reduce the effect of albedo and crosstalk in every color channel. To cope with this, a previous color calibration has been pursued. This procedure uses least squares to find the matrix that best linearises the projector-camera pair in terms of response to color intensity, for each color channel (red, green and blue). This linear transformation is extracted for every pixel in the image, providing an estimation of the projected color values for every received value. Having the set of three received color values R, G, B the estimated projected values R, G, B are given by eq.(10):

$$\begin{bmatrix} R_0 \\ G_0 \\ B_0 \end{bmatrix} = \begin{bmatrix} a_{rr} & a_{rg} & a_{rb} \\ a_{gr} & a_{gg} & a_{gb} \\ a_{br} & a_{bg} & a_{bb} \end{bmatrix} \begin{Bmatrix} R \\ G \\ B \end{Bmatrix} \quad (10)$$

This matrix represents the whole system (projector-camera) and aims to substract the effect of crosstalk between color channels. However, as it approximates the system as a linear transformation between projected and received images, some errors will persist due to non-linearities. This error, jointly with the different albedo and noise, must be filtered by the wavelet analysis algorithm. The wavelet analysis employs a 2D wavelet decomposition using a Morlet mother wavelet. As stated in [1],

Morlet wavelet is optimal in case we deal with signal having a low Signal To Noise ratio, which is the case when working in real conditions. Moreover, 2D wavelet analysis performs better than 1D wavelet analysis. In our case, a 2D wavelet decomposition and phase estimation algorithm combined with cost function is employed. The output of the 2D wavelet analysis is a 5D matrix of dimensions $height \cdot width \cdot scales \cdot translations \cdot orientations$. Without the cost function, the algorithm would select for every pixel the daughter wavelet having the maximum of the modulus -within all scales, translations and orientations available-, and its corresponding angle for that position. The cost function is introduced to ensure continuity and avoid errors due to local errors, that can be identified regarding its neighbours. The cost function works along the y axis of the camera (though any other direction could be selected according to the direction of fringes in the projected pattern), selecting the combination of daughter wavelet that best performs in terms of modulus maxima and continuity. The algorithm used by the cost function is presented in eq.(11):

$$Cost = \sum_{W}^{b=2} \{-|S[\phi(b), b]|^2 + |\phi(b) - \phi(b-1)|^2\} \quad (11)$$

where $\phi(b)$ represents any value of the scaling parameter, b is the shifting parameter in the coding axis (y axis in our case), $S[\phi(b), b]$ is the modulus value at both $\phi(b)$ and b, and W is the total width of the fringe pattern, in pixels. For every column, the algorithm works at follows:

- Compute all the possible daughter wavelets, for every orientation.
- For every orientation and every value of the shifting parameter b, selects the best path in terms of:
  - Maxima of the modulus (to maximize).
  - Difference in scale value with respect to the previous position in the path (to minimize).
- Finally, selects the orientation having the lowest global cost.

This procedure reduces the errors in presence of local holes in the recieved fringe pattern. Once the appropiate daughter wavelets have been selected, their correspoding angle values are computed and the wrapped phase map is extracted. The next step is to apply the unwrapping algorithm of absolute coding proposed above. A minimum of two patterns are required to this end, but the proposed method utilizes the three color channels (red, green and blue) to create the absolute phase map. This is done to increase the redundancy and hence reduce the errors that may propagate to the absolute phase map. The algorithm combines every two of the color channels to create an absolute phase map. That is, a total of $\binom{n}{2}$ combinations are created, being $n = 3$ the number of channels. An absolute phase map is computed for every one of the combinations following the idea of relative phase numbers exposed above.

Consistency mapping

Once these absolute maps are computed, an optimization algorithm is pursued to extract the optimal phase map that minimizes the errors. This process is done in order to reduce the noise created by the effect of non linearities of the projector-camera pair in color or intensity representation. This noise propagates from the wrapped phases to the absolute phase map. The optimization algorithm detects these noisy points or regions and replace them with a non-corrupted value coming from another pre-computed absolute phase map. The algorithm works as follows:

1. The laplacian map of every absolute phase map is computed, and the one having the lowest mean value of laplacian is chosen as the default map.
2. Every pixel having a laplacian value higher than the computed mean is selected to revision. This pixel is substituted by the one that minimizes the mean of laplacians, among all the possibilities provided by the absolute phase maps.

This process suppress the error provided by isolated pixels having a value much different from the neighbouring pixels.

5. Results

The proposed algorithm has been tested in both simulated and real environment, and the resulting reconstruction are shown herebelow. The setup used for the tests was composed of an LCD video projector (Epson EMP-400W) with a resolution of 1024×768 pixels, a camera (Sony 3CCD) and a frame grabber (Matrox Meteor-II) digitizing images at 768×576 pixels with 3×8 bits per pixel (RGB). The baseline between camera and projector was about $0.5m$. The results and time estimates were computed using a standard Intel Core2 Duo CPU at 3.00GHz. The selected frequencies for the three fringe pattern were $p = 15$, $p = 19$ and $p = 23$ periods. These values provide a good resolution in details, while preserving the sinusoidal shape once captured by the camera.

5.1. Simulated results

The proposed algorithm was tested using simulated data. The *peak* function available in Matlab (shown in Fig. 5) has become a benchmark for fringe pattern analysis, as stated in [16], as was employed for the test. Moreover, the simulated

object shape was obtained for different values of noise. The error introduced is a gaussian zero mean random noise in the range 5%, 10% and 20% of the total dynamic range of input image. The resulting patterns used as input images are shown in Fig. 6.

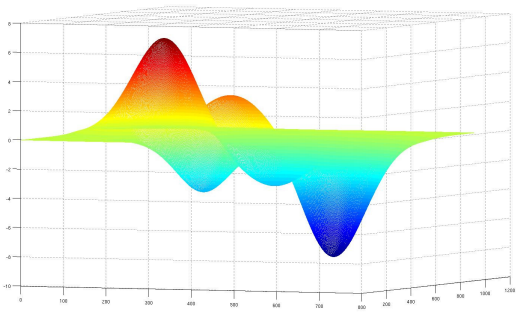

Figure 5: Projected simulated object shape

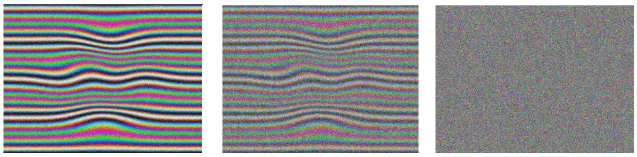

(a) Noise 5% (b) Noise 10% (c) Noise 20%

Figure 6: Input images for added noise values of 5%, 10% and 20% of maximum dynamic range, respectively

The reconstructed object shape obtained using the input image of noise 5% of the total range are shown in Fig. 7a. As can be observed, the algorithm reconstructs the simulated object at the same time the noise existing in the input image is reduced. A scaled map of the error is also presented in Fig. 7b, where the error has been rescaled from $[0\%, 3.48\%]$ to $[0, 255]$. The error is uniformly distributed, with some peaks in the regions of major inclinations of the *peak* function. This is due to the fact that a faster change in the phase frequency is more likely to suffer detection errors when noise appears. The algorithm was also tested with the other noised input images, and the results of average error are presented in table 1. The error is highly reduced for values lower than 5% of the data range, up to values higher than 20% of data range which makes the decoding impossible. It is important to note that noise introduced depends on the object depth. For the object depths analyzed in real applications the noise remains under 5% of this dynamic range, and hence the method is able to filter the noise in the reconstructed shape, as will be observed in the experimental results.

Finally, in order to test the effectivity of the proposed

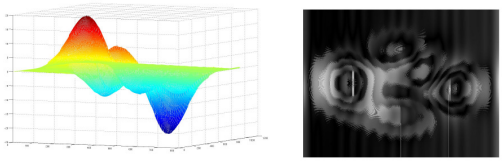

(a) Reconstructed object. (b) Scaled error map.

Figure 7: Reconstructed peak model with 5% noise, and corresponding error map rescaled from $[0\%, 3.48\%]$ to $[0, 255]$.

Noise percentage $(\%)$	**Error rate** $(\%)$
5	0.57
10	19,8
20	—

Table 1: Error rates for the given input noise, goin from 5% to 20% of the total dynamic range.

method against situations like the one shown in Fig 1, a reconstruction of this setup has been simulated. The effectivity of the absolute coding step used in the proposed algorithm is shown in Fig 8. The slope has been detected despite it was not visually perceptible. However, some error arised in the vecinity of the discontinuity, due to the erroneous phase estimation in the surroundings of the slope. This problem is posteriorly analyzed.

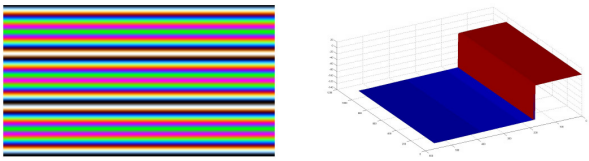

Figure 8: Projected and reconstructed simulated surface containing a slope

5.2. Experimental results

The proposed technique was tested under real conditions, for the reconstruction of two different objects: a smooth volume done with sheets of paper having different orientations, and a plaster white face. These two objects attemp to cover the usual requirements of the methods regarding its applicability to 3D dense reconstruction. It is important to note that this objects have been chosen having lambertian white surfaces, in order fit with the previous color calibration performed to the system. The results are presented in Figs. 10,12.

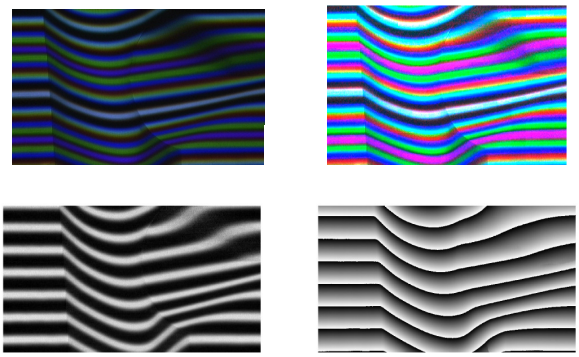

Figure 9: Real smooth object: recovered image, enhanced image, one color channel and its wrapped phase

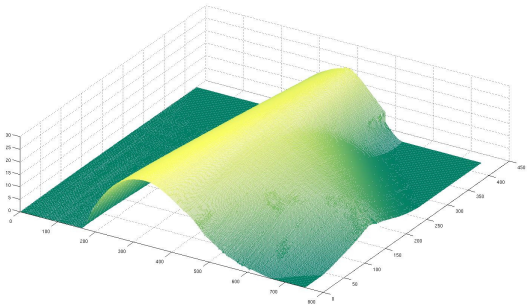

Figure 10: Reconstructed surface of the smooth object

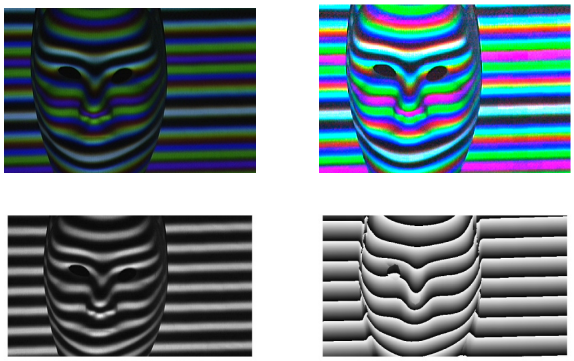

Figure 11: Real white face: recovered image, enhanced image, one color channel and its wrapped phase

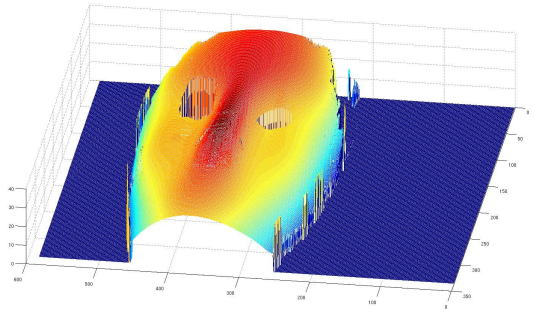

Figure 12: Reconstructed surface of the white face

The flat plane that surrounds the scanned objects has been reconstructed with absolutely no error. This is due to the Morlet mother wavelet used to extract the phase, which is optimal in case of having low signal to noise ratio. The smooth surface is reconstructed also without error, not depending on the orientation and shape of the object. Finally, the algorithm is able to reconstruct the face providing a dense absolute coding reconstruction using one single projection. As can be observed, the main volume has been detected and details like the nose and eyes (identified as shadows) are represented in the final surface. A more detailed features like the nose can be achived increasing the frequency of the projected fringes. However, a camera having greater resolution would be needed to preserve the sinusoidal shape of the recovered patterns. The reconstruction presents, however, some errors in the discontinuities (see Fig.12), the same kind of error that revealed in the simulated results. This problem is due to an inaccurate phase extraction in the wavelet analysis step, which originates an erroneus phase estimation at the vecinity of the discontinuity, which propagates to the absolute phase map. This problem was mentioned in the work of [1] as the major drawback of the wavelet technique employed in this algorithm. Regarding this issue, some improvements are being implemented using an adaptive selection of the best mother wavelet, in both type and shape, depending on the proximity to a discontinuity. Having this, the method provides an absolute coding dense reconstruction technique able to deal with moving scenarios, extending the applicability of structured light to dynamic environment requiring high level of detail in the reconstructed shape.

6. Conclusion

In this work, we have presented a one-shot dense reconstruction technique for structured light. Moreover, an absolute coding phase unwrapping algorithm has been proposed, suppressing errors due to a bad detection of slopes and error propagation between pixels during the unwrapping step.

The work is based on the multiplexation in color space of three different fringe patterns. The phase of these patterns is extracted using wavelet decomposition combined with a cost function algorithm. The final step merges the individual relative phase maps to create the absolute phase map and extract the depth deviation. The algorithm has been tested in both simulated and real data. The results show the effectiviness of the proposed method using standard simulation parameters. The method reconstruct properly smooth surfaces in real data. However, some problems were encountered with surfaces having discontinuities. This is due to the effect of the phase changes when selecting the best phase value for a pixel in the discontinuity. The solution pointed out in this paper focuses on adapting the shape or even the type of the mother wavelet depending on the proximity to a discontinuity, so as to be able to obtain the correct relative phase for all the pixels in the image and hence produce dense reconstruction of objects in movement without ambiguities in depth.

References

[1] A. Z. A. Abid. Fringe Pattern Analysis using Wavelet Transforms. Master's thesis. 3, 4, 7

[2] A. Baldi, F. Bertolino, and F. Ginesu. On the performance of some unwrapping algorithms. *Optics and Lasers in Engineering*, 37(4):313–330, 2002. 3

[3] B. Carrihill and R. Hummel. Experiments with the intensity ratio depth sensor. *Computer Vision, Graphics, and Image Processing*, 32(3):337–358, 1985. 1

[4] W. Chen, P. Bu, S. Zheng, and X. Su. Study on Fourier transforms profilometry based on bi-color projecting. *Optics and Laser Technology*, 39(4):821–827, 2007. 2

[5] F. Forster. A High-Resolution and High Accuracy Real-Time 3D Sensor Based on Structured Light. In *Proc.3th International Symposium on 3D Data Processing, Visualization, and Transmission*, pages 208–215, 2006. 1

[6] M. Gdeisat, D. Burton, and M. Lalor. Eliminating the zero spectrum in Fourier transform profilometry using a two-dimensional continuous wavelet transform. *Optics Communications*, 266(2):482–489, 2006. 2, 3

[7] P. Huang, S. Zhang, F. Chiang, et al. Trapezoidal phase-shifting method for three-dimensional shape measurement. *Optical Engineering*, 44:123601, 2005. 1

[8] J. Li, X. Su, and L. Guo. Improved Fourier transform profilometry for the automatic measurement of three-dimensional object shapes (Journal Paper). *Optical Engineering*, 29(12):1439–1444, 1990. 2

[9] J. Lin and X. Su. Two-dimensional Fourier transform profilometry for the automatic measurement of three-dimensional object shapes. *Optical Engineering*, 34:3297–3297, 1995. 2

[10] S. Mallat. *A Wavelet Tour of Signal Processing*. AP Professional, London, 1997. 3

[11] R. Morano, C. Ozturk, R. Conn, S. Dubin, S. Zietz, and J. Nissano. Structured light using pseudorandom codes. *IEEE Transactions on Pattern Analysis and Machine Intelligence*, 20(3):322–327, 1998. 1

[12] J. Pages, J. Salvi, C. Collewet, and J. Forest. Optimised De Bruijn patterns for one-shot shape acquisition. *Image Vision and Computing*, 23:707–720, 2005. 1

[13] T. Pribanic, H. Dapo, and J. Salvi. Efficient and Low-Cost 3D Structured Light System Based on a Modified Number-Theoretic Approach. *EURASIP Journal on Advances in Signal Processing, In Press, doi:10.1155/2010/474389*, 2009. 2, 3

[14] P. Ribenboim. *Algebraic numbers*. R. Courant, L. Bers, J.J. Stoker. John Wiley and Sons. New York, 1972. 3

[15] J. Salvi, J. Batlle, and E. Mouaddib. A robust-coded pattern projection for dynamic 3D scene measurement. *Pattern Recognition Letters*, 19(11):1055–1065, 1998. 1

[16] J. Salvi, S. Fernandez, T. Pribanic, and X. Llado. A state of the art in structured light patterns for surface profilometry. *Pattern recognition, in Press, doi:10.1016/j.patcog.2010.03.004*, 2010. 1, 3, 5

[17] J. Salvi, J. Pages, and J. Batlle. Pattern codification strategies in structured light systems. *Pattern Recognition*, 37(4):827–849, 2004. 1

[18] V. Srinivasan, H. Liu, and M. Halious. Automated phase-measuring profilometry: a phase mapping approach. *Applied Optics*, 24:185–188, 1985. 1

[19] J. Tajima and M. Iwakawa. 3-D data acquisition by rainbow range finder. In *Pattern Recognition, 1990. Proceedings., 10th International Conference on*, volume 1, 1990. 1

[20] M. Takeda M, Mutoh. Fourier transform profilometry for the automatic measurement of 3-D object shapes. *Appl. Opt*, 22:3977–3982, 1983. 2

[21] L. Wu and Q. Peng. Research and development of fringe projection-based methods in 3D shape reconstruction. *Journal of Zhejiang University-Science A*, 7(6):1026–1036, 2006. 3

[22] H. Yue, X. Su, and Y. Liu. Fourier transform profilometry based on composite structured light pattern. *Optics and Laser Technology*, 39(6):1170–1175, 2007. 2